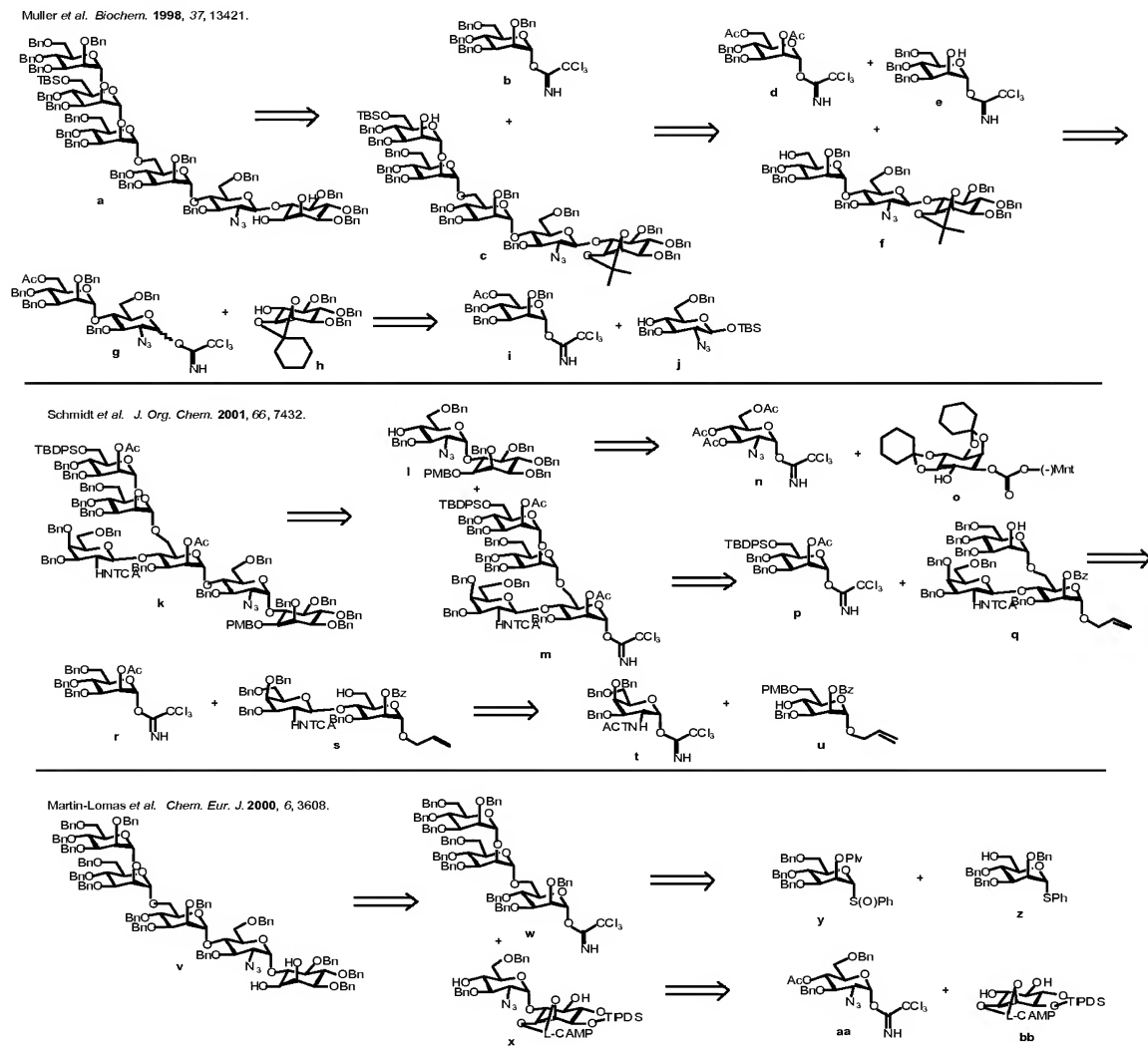


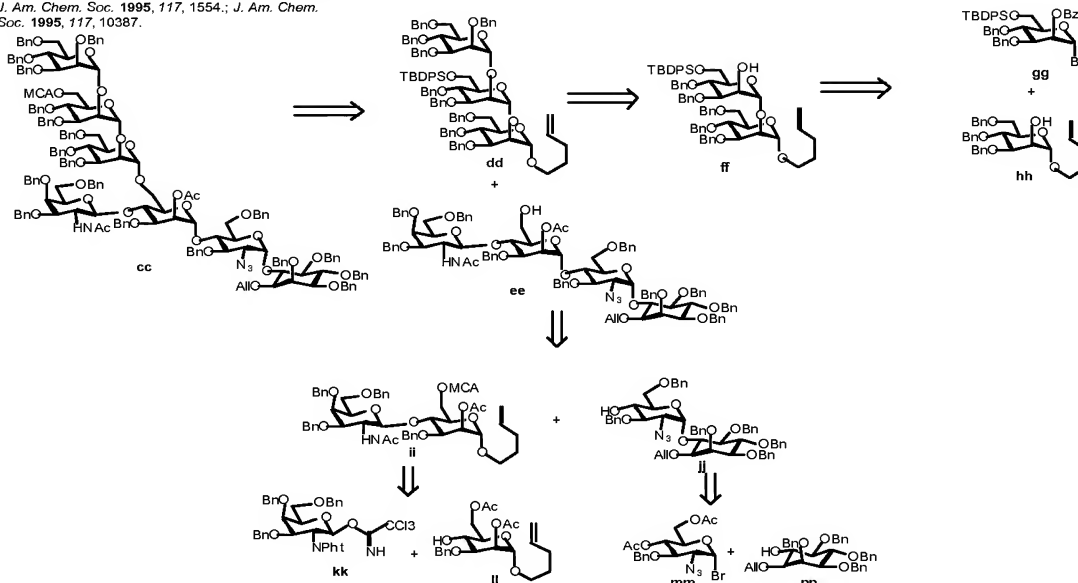
# *In the Specification*

On page 2, please delete the illustration reproduced below:

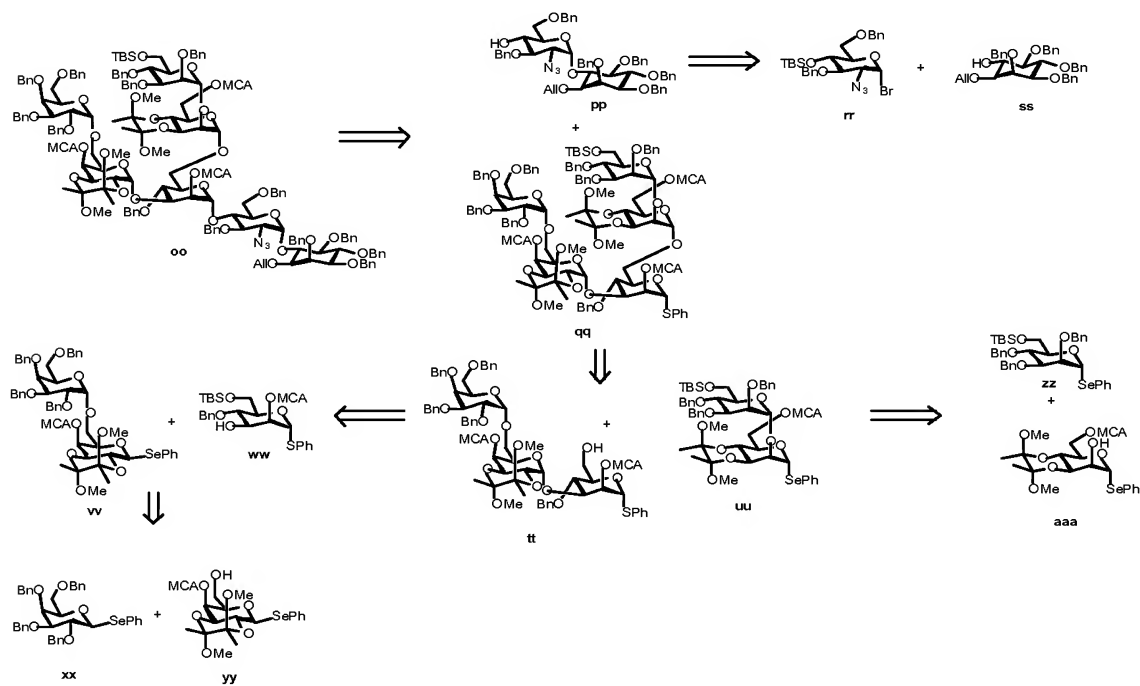


On page 3, please delete the illustration shown below:

Fraser-Ried *et al.* *J. Am. Chem. Soc.* **1993**, *115*, 7886;  
*J. Am. Chem. Soc.* **1995**, *117*, 1554.; *J. Am. Chem.*  
*Soc.* **1995**, *117*, 10387.



Ley *et al.* *Chem. Eur. J.* **2000**, *6*, 172.



Please amend page 3, lines 3-7, as follows:

Müller *et al.* have reported a synthesis using **a**.<sup>10</sup> See Figure 1A and Figure 1B. This route is non-convergent, making modification more difficult; it suffers from a ~~dependance~~ dependence on protecting-group manipulations on large structures, which results in loss of more valuable material; and the protecting-group combinations used (esp. the TBS and isopropylidene) are incompletely orthogonal and restrict the diversity of structures possible.

Please amend page 4, lines 1-19, as follows:

Schmidt *et al.* have reported a method using **k**.<sup>11</sup> See Figure 2A and Figure 2B. This synthesis, much like the one mentioned previously, shows some similarity to our methods, indicating a limited degree of ~~concensus~~ consensus among GPI chemists. See the extended commentary, *infra*, for analysis.

Martín-Lomas *et al.* used **v** as an intermediate.<sup>10</sup> See Figure 3. Their method uses a variety of protecting group-patterns requiring late-stage manipulation; it also lacks the flexibility to install phosphate moieties in the natural manner (or at all), thus limiting the utility for making structures recognized by biological systems.

Fraser-Reid *et al.* have made **cc**, which incorporates many robust and generally useful protecting-group patterns.<sup>12</sup> See Figure 4A and Figure 4B. The principal drawback to this route is the near-exclusive use of *n*-pentenyl glycoside donors, developed by the group; although these do provide acceptable results, their lack of adoption by the carbohydrate-synthesis community at large is testament to the difficulty of applying them successfully. Our method uses more common techniques which are reliable even when applied by less-skilled operators.

Similarly, many of the protection schemes used by Ley *et al.* in **oo** are intended to demonstrate a new technology rather than produce optimal results or versatility.<sup>8</sup> See Figure 5. Although the generation of large structures is possible, our simple, general methods provide greater opportunities for easy modification of the synthesis, minimize the chances of protecting-group ~~incompatibility~~ incompatibility, and make deprotection of the final structures simpler.

Please add the following paragraphs on page 5, between lines 5 and 6 (*i.e.* immediately before the “Detailed Description of the Invention” section):

***Brief Description of the Figures***

**Figures 1A and 1B** depict a retrosynthesis from Muller *et al. Biochem.* **1998**, 37, 13421.

**Figures 2A and 2B** depict a retrosynthesis from Schmidt *et al. J. Org. Chem.* **2001**, 66, 7432.

**Figure 3** depicts a retrosynthesis from Martin-Lomas *et al. Chem. Eur. J.* **2002**, 6, 3608.

**Figure 4A and 4B** depict a retrosynthesis from Fraser-Reid *et al. J. Am. Chem. Soc.* **1993**, 115, 7886; *J. Am. Chem. Soc.* **1995**, 117, 1554; and *J. Am. Chem. Soc.* **1995**, 117, 10387.

**Figure 5** depicts a retrosynthesis from Lay *et al. Chem. Eur. J.* **2000**, 6, 172.

**Figure 6** depicts a *P. falciparum* GPI (1).

**Figure 7** depicts a potential GPI anti-toxin vaccine 3.

**Figure 8** depicts a retrosynthesis of GPI 2.

**Figure 9** depicts a synthesis of inositol acceptors.

**Figure 10** depicts a synthesis of a glucosamine building block.

**Figure 11** depicts a synthesis of trichloroacetimidate building blocks.

**Figures 12A and 12B** depict a first generation synthesis.

**Figure 13** depicts alternative hydrolysis conditions.

**Figure 14** depicts a model trisaccharide synthesis.

**Figure 15A and 15B** depict asynthesis of cyclic phosphate.

**Figure 16** depicts a synthesis of target 2.

**Figure 17 and 18** depict a preparation of immunogen and sham.

**Figure 19** shows that immunization against the synthetic GPI glycan substantially protects against murine cerebral malaria, pulmonary edema and acidosis. a) Kaplan-Meier survival plots, and b) parasitaemias, to 2 weeks post-infection, of KLH-glycan-immunized (closed circles) and sham-immunized (open squares) mice challenged with *P. berghei* ANKA; c)

As an index of pulmonary edema, the ratio of wet weight to dry weight of lungs from KLH-glycan-immunized and sham-immunized animals at day 6 post-infection are expressed as a proportion of the lung wet:dry weight ratio of age/sex matched uninfected controls; and d) pH of serum drawn at day 6 from uninfected and *P. berghei*-ANKA-infected immunized and sham-immunized donors.

**Figure 20A and 20** depict a retrosynthesis for automated synthesis.

**Figure 21** depicts an automated synthesis of GPI **46**.

**Figure 22** depicts a table showing conditions for automated synthesis of **46**.

**Figure 23** depicts an HPLC analysis of automated synthesis of **46**. Flow rate: 1 mL/min, 5→20% EtOAc/hexanes (20 min).

**Figure 24** depicts a 4+2 coupling.

**Figure 25** depicts differentially-protected disaccharide acceptors.

**Figure 26** depicts a solution-phase synthesis of tetramannose structure.

**Figure 27A and 27B** depict a synthesis of more-versatile tetramannose donor.

Please amend page 6, lines 11-21, as follows:

Anti-toxin vaccines target the toxin that is released following erythrocyte rupture, and represent the second form of protection against blood-stage parasites. Release of this toxin is thought to initiate an inflammatory cascade in the host, resulting in the release of harmful cytokines such as tumor necrosis factor (TNF $\alpha$ ). An effective anti-toxin vaccine would prevent the inflammatory cascade in the host through antibody sequestration and neutralization of the parasite toxin; as the cascades caused by the toxin are necessary for parasite success, evolved resistance should be blunted. A GPI of parasite origin (**1**) was recently isolated that induced several of the pathological effects associated with severe malaria and was thus a candidate toxin (~~Figure 4.1~~ Figure 6).<sup>15</sup> Purified GPI induced TNF $\alpha$  expression and NO output in macrophages, both of which occur during real infections and lead to clinical manifestations of malaria.

On page 6, please delete the illustration and caption shown below:

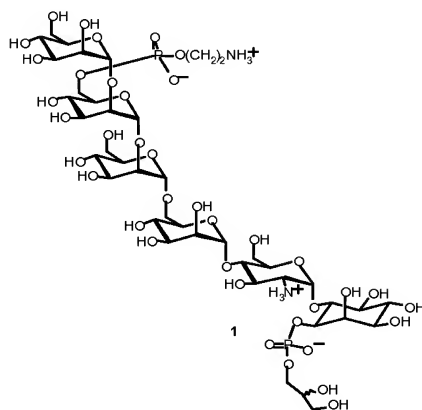


**Figure 4.1** *P. falciparum* GPI

Please amend page 7, lines 3-8, as follows:

What remained to be established was if an anti-toxin vaccine based on the structure of the isolated GPI would reduce pathogenesis or fatalities in any disease condition. Anti-toxin vaccines have been discussed for some time,<sup>17</sup> but never reduced to practice. We sought to determine whether immunization with GPI oligosaccharide fragment **3**, prepared by chemical synthesis, could prevent pathology and fatalities in a rodent model of severe malaria (~~Figure 4.2~~ Figure 7).

On page 7, please delete the illustration and caption shown below:

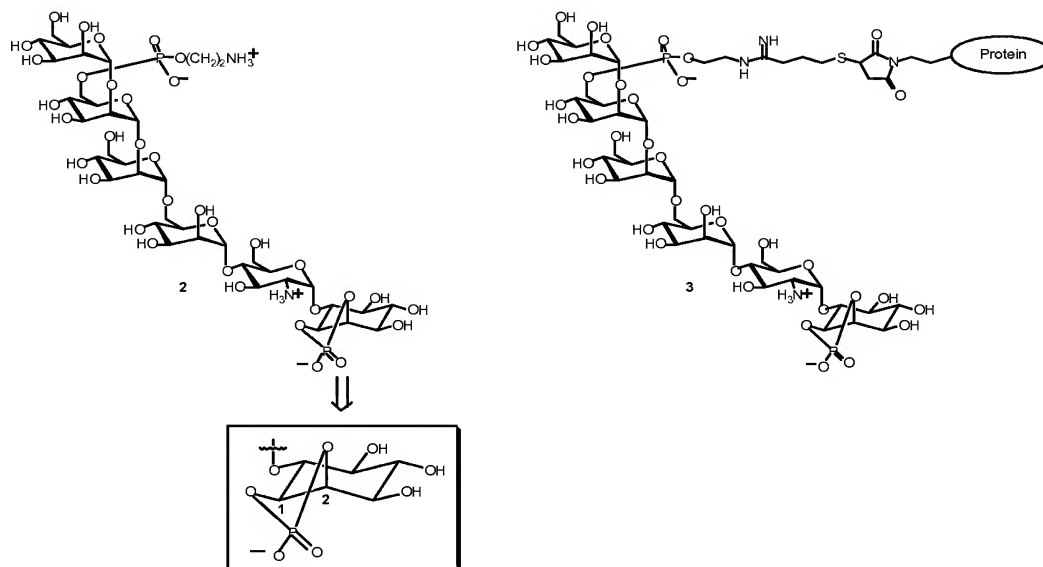


**Figure 4.2** Potential GPI anti-toxin vaccine **3**

Please amend page 7, line 21, to page 8, line 2, as follows:

We developed a synthetic route for **2** that employed five differentially-protected glycosyl donors, one inositol and one phosphoramidite building block (~~Figure 4.3~~ Figure 8). While the initial synthesis of **2** was carried out in solution, our ultimate goal was automated solid-phase synthesis,<sup>19</sup> which helped guide our selection of protecting groups and glycosyl donors.

On page 8, please delete the illustration and caption shown below:

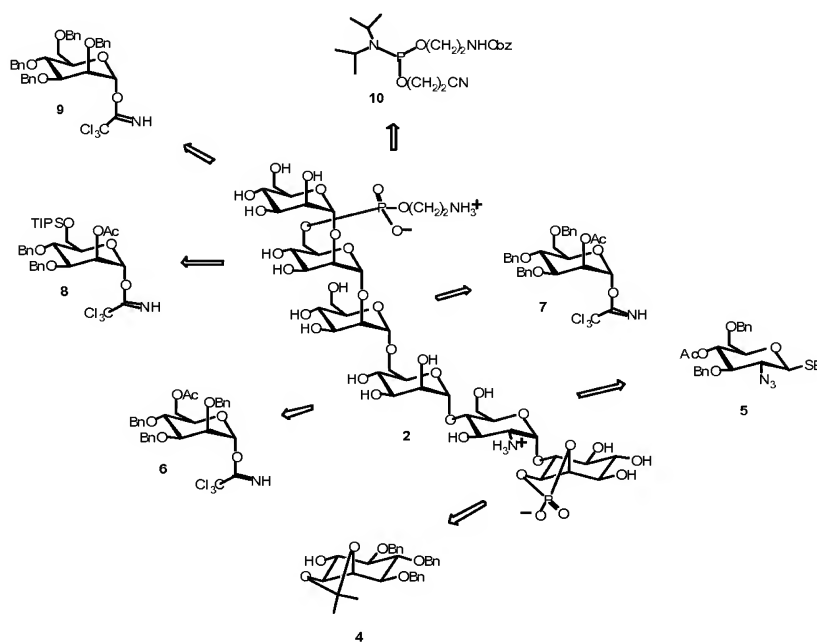


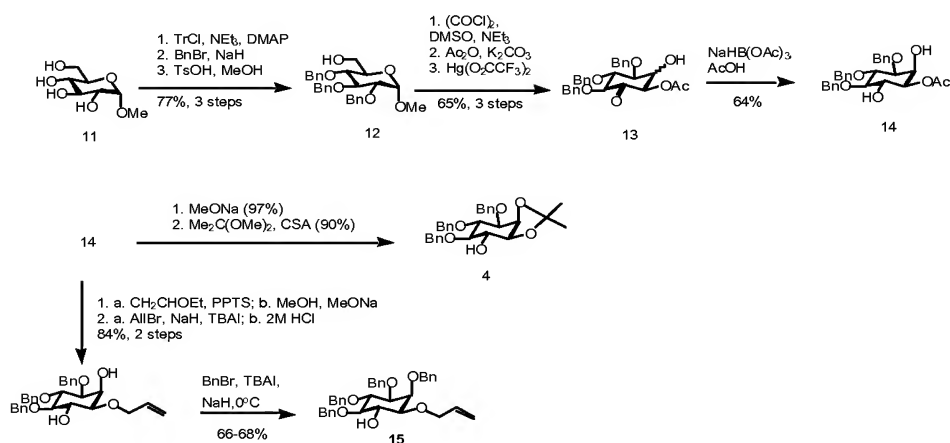
**Figure 4.3** Retrosynthesis of GPI **2**



Please amend page 8, lines 6-18, as follows:

Building blocks **4**,<sup>20</sup> **7**,<sup>7a</sup> **9**,<sup>7a</sup> and **10**<sup>7b</sup> were prepared following known procedures, while thiodonor **5** and imidates **6** and **8** required novel syntheses. The route to myo-inositol acceptor **4** (Scheme 4.1 Figure 9) followed literature precedent.<sup>20a</sup> Selective mono tritylation<sup>21</sup> of the methyl- $\alpha$ -D-glucopyranoside **11** followed by benzylation and removal of the temporary trityl ether gave **12**. Swern oxidation,<sup>22</sup> formation of a mixture of isomeric enol acetates ( $\text{Ac}_2\text{O}$ ,  $\text{K}_2\text{CO}_3$ ), and Ferrier reaction<sup>23</sup> under the catalysis of mercuric acetate provided hydroxy-ketone **13** in 53% for 3 steps. Internal-delivery reduction with sodium triacetoxyborohydride gave the *anti* diol in 64% yield. Cleavage of the acetate with  $\text{NaOMe}/\text{MeOH}$  provided a known triol,<sup>23</sup> and protection of the *cis* alcohols as their isopropylidene under thermodynamic control gave acceptor **4**. Alternatively, protection of the hydroxyls of diol **14** as ethoxyethyl ethers, replacement of acetyl by allyl, and removal of the acetals allowed production of differentiated acceptor **15**. This molecule should allow use of non-cyclic phosphodiester.

On page 9, please delete the illustration and caption shown below:

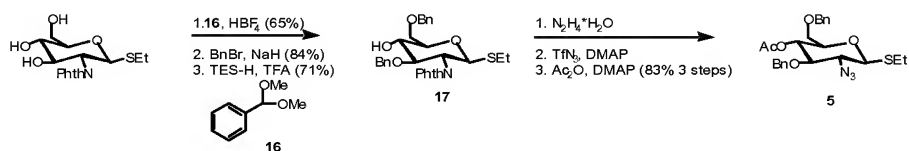


**Scheme 4.1** Synthesis of inositol acceptors

Please amend page 9, lines 4-16, as follows:

For preparation of glucosamine building block **5**, we started from known phthalimide-protected triol<sup>25</sup> (~~Scheme 4.2~~ Figure 10). Protection of the 4,6-diol as a benzylidene ring proceeded under the agency of tetrafluoroboric acid<sup>26</sup> in 65% yield, followed by benzylation of the remaining alcohol (84% yield). Regioselective opening of the benzylidene using triethylsilane and trifluoroacetic acid<sup>27</sup> afforded 3,6 di-benzyl thioglycoside **17** in 71% yield. The next transformation *en route* to the desired donor was an amine protecting group switch, from phthalamide to azide. Phthlamide groups are not compatible with the conditions used for cleavage of acetate esters (*vide infra*), and would also favor an undesirable  $\alpha$ -linkage in the initial coupling event. Cleavage of the phthlamide with hydrazine monohydrate was followed by treatment of the crude amine with freshly prepared triflic azide.<sup>28</sup> Treatment of the crude product with acetic anhydride and DMAP followed by chromatography provided thiodonor **5** in 83% yield for the three steps.

On page 9, please delete the illustration and caption shown below:

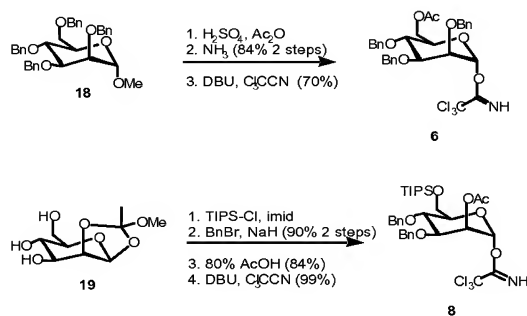


**Scheme 4.2** Synthesis of glucosamine building block

Please amend page 9, line 21, to page 10, line 6, as follows:

The synthesis of imidate **6** began with per-benzylated methyl mannopyranoside **18**<sup>29</sup> (Scheme 4.3 Figure 11). Conversion of both the anomeric methoxy group and the 6-O-benzyl group to acetates was accomplished using concentrated sulfuric acid with acetic anhydride as solvent.<sup>30</sup> The anomeric acetate was cleaved using ammonia, and the resulting lactol was converted into trichloroacetimidate<sup>31</sup> **6** using trichloroacetonitrile and catalytic DBU. The additional degree of orthogonality required of building block **8** necessitated the use of orthoester **19**.<sup>32</sup> Regioselective protection of the 6-position as a silyl ether was followed by dibenzylation in 90% yield over two steps. Aqueous acetic acid was employed for the opening of the orthoester (82%), resulting in formation of a 2-O-Ac anomeric lactol. Preparation of imidate **8** proceeded in high yield using trichloroacetonitrile and DBU.

On page 10, please delete the illustration and caption shown below:

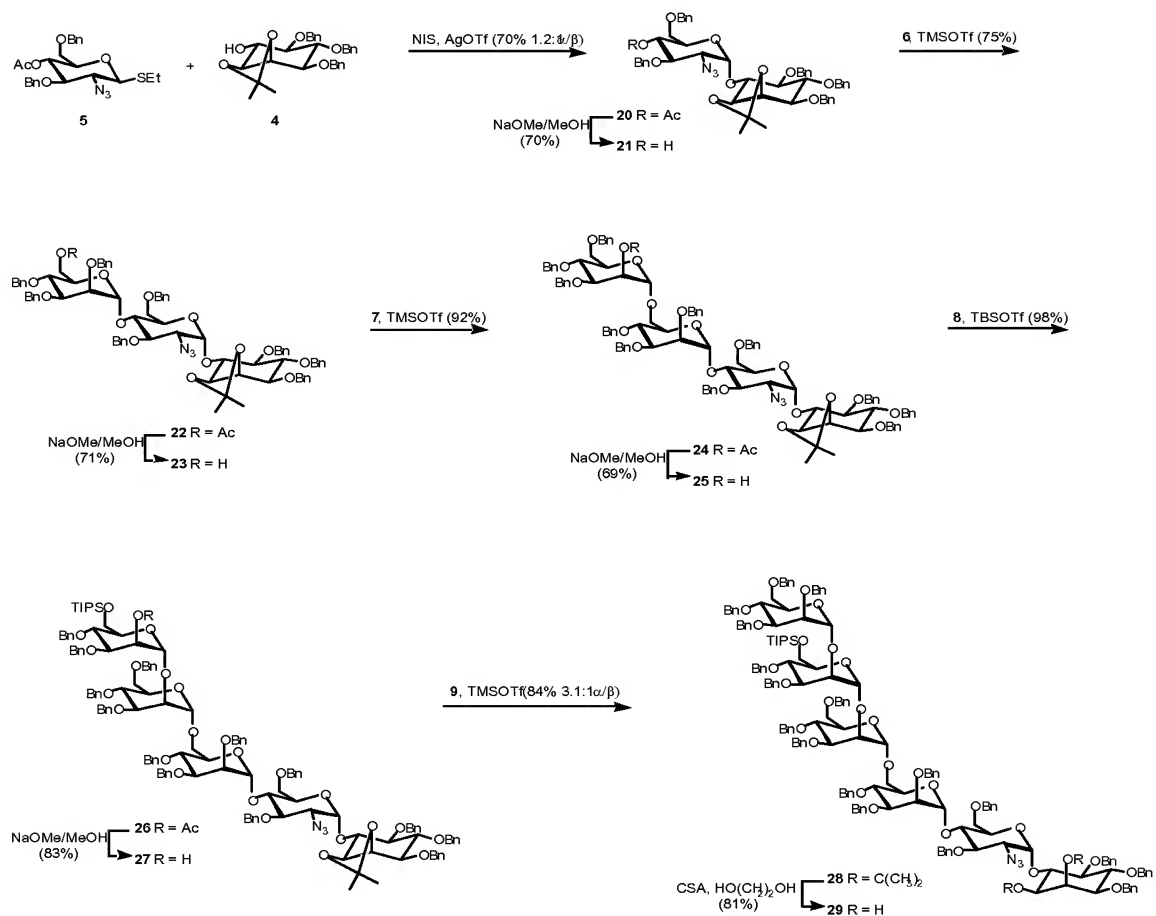


**Scheme 4.3** Synthesis of trichloroacetimidate building blocks

Please amend page 10, lines 11-28, as follows:

The first glycosidic linkage to be formed was the difficult union between thiodonor **5** and inositol derived acceptor **4** (~~Scheme 4.4~~ Figure 12A and Figure 12B). Activation with *N*-iodosuccinimide/silver triflate provided pseudo-disaccharide product **20** in 70% yield as a separable 1.2:1 mixture in favor of the desired  $\alpha$ -isomer. Deprotection with sodium methoxide removed the acetyl group to give acceptor **21**, which was then coupled to trichloroacetimidate **6** in 75% yield. Cleavage of the acetate of the resultant pseudo-trisaccharide **22** provided acceptor **23**, which was positioned for the next coupling with building block **7**. This coupling proceeded in high yield (92%) and furnished exclusively  $\alpha$ -linked pseudo-tetrasaccharide acceptor **25** following deprotection with sodium methoxide in methanol. Coupling of acceptor **25** and donor **8** proceeded in excellent yield under slightly milder conditions (TBSOTf), and was followed by deprotection to give pseudo-pentasaccharide acceptor **27**. The addition of a terminal mannose subunit proceeded in high yield (84%) with donor **9**, but afforded a mixture of anomers that were inseparable by silica gel chromatography. Deprotection of the isopropylidene acetal<sup>7b</sup> on the inositol ring proved to be a difficult transformation, providing mixtures of starting material, desired diol **29**, and triol arising from concomitant TIPS cleavage. After multiple recycling steps and tedious column chromatography **29** was isolated in a modest yield of 67%, albeit still as a mixture of isomers from the 5+1 coupling event.

On page 11, please delete the illustration and caption shown below:

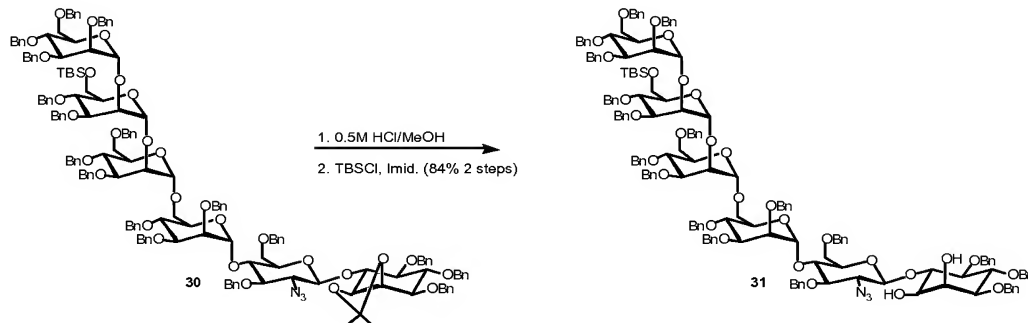


**Scheme 4.4** First generation synthesis

Please amend page 11, lines 5-13, as follows:

The difficulties encountered in the final coupling event and problematic hydrolysis of the isopropylidene group prompted us to explore an alternate route to a protected diol such as **29**. Replacing per-benzylated donor **9** with 2-acetate donor **7** would be a straightforward solution to the first problem. Following saponification and benzylation the protected pseudo-hexasaccharide should be isolable as a single isomer. For a solution to the sluggish hydrolysis reaction, we turned to an earlier GPI synthesis by Frick *et al.*<sup>10a</sup> Instead of trying to prevent concomitant silyl ether cleavage in the course of acetal cleavage, the authors had hydrolysed all acid labile groups (**Scheme 4.5** **Figure 13**). After workup, the silyl ether had been regioselectively re-installed on the primary alcohol to give **31**.

On page 12, please delete the illustration and caption shown below:

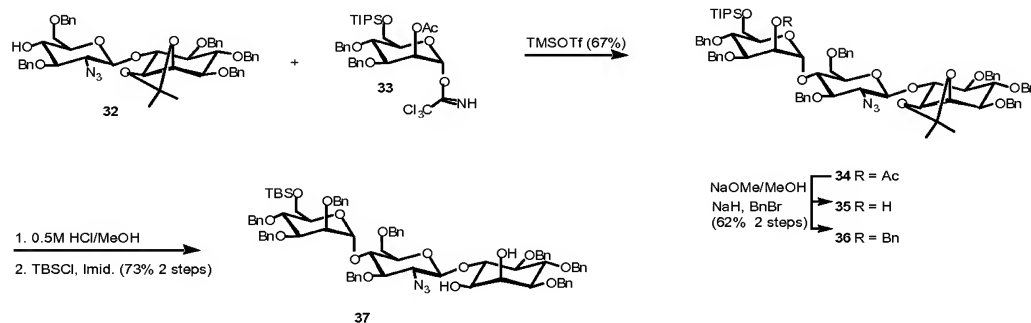


**Scheme 4.5** Alternative hydrolysis conditions

Please amend page 12, lines 4-12, as follows:

A model trisaccharide bearing the appropriate functionality was constructed to examine the hydrolysis reaction (~~Scheme 4.6~~ **Figure 14**). Disaccharide acceptor **32** was reacted with donor **33** to give a 67% yield of desired pseudo-trisaccharide **34**. Saponification and benzylation proceeded smoothly in a combined 62% yield for the two steps, and set the stage for the model hydrolysis. Hydrolysis of the TIPS ether and isopropylidene groups was accomplished using 0.5 M HCl in methanol over 12 hours, followed by alkaline workup. Following reaction with TBS-Cl and imidazole (imid.), a 73% yield of desired diol **37** was isolated. The good yield of the model reaction coupled with its operational simplicity prompted us to apply these hydrolysis conditions.

On page 12, please delete the illustration and caption shown below:



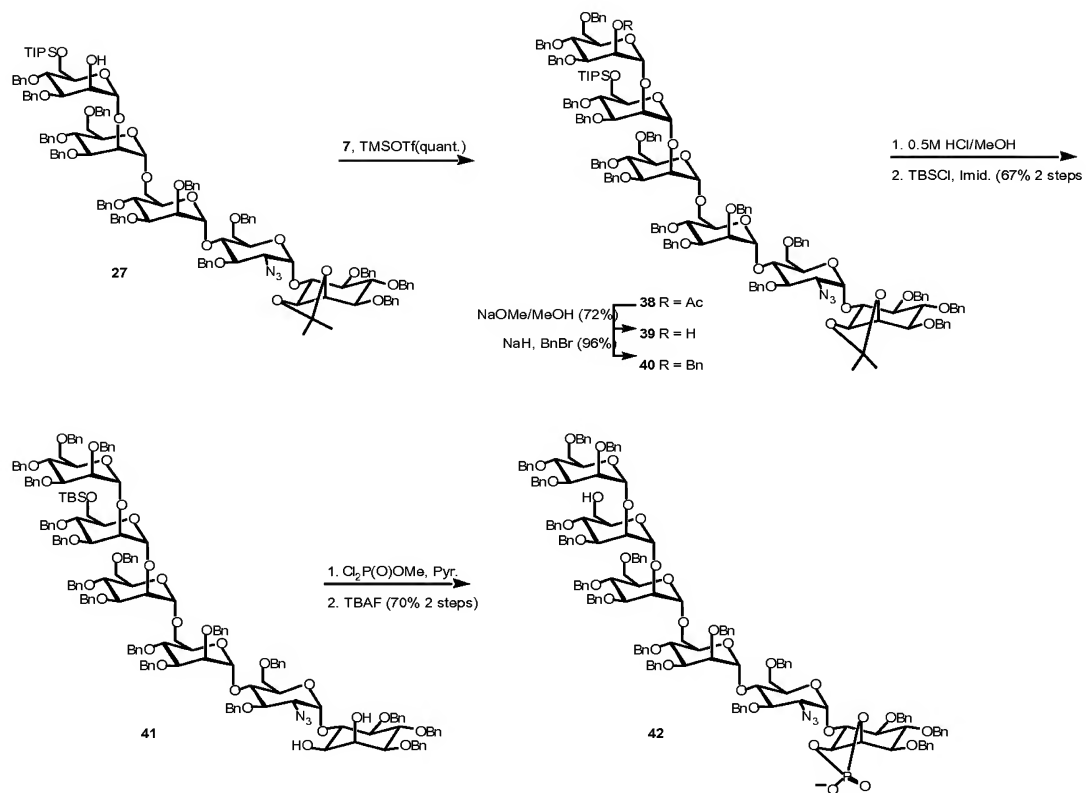
**Scheme 4.6** Model trisaccharide synthesis

Please amend page 12, line 17, to page 13, line 3, as follows:

Starting from pseudo-pentasaccharide acceptor **27**, 2-Ac donor **7** was installed to give a quantitative yield of the desired pseudo-hexasaccharide as a single isomer (~~Scheme 4.7~~ Figure 15A and Figure 15B). The structure of **38** was confirmed using several 2D-NMR experiments (COSY, HSQC, HMBC, TOCSY).<sup>33</sup> Deprotection gave a 72% yield of the pseudo-hexasaccharide **39** before benzylation afforded compound **40** in 96% yield. Following the conditions used for our model trisaccharide, hydrolysis and re-installation of the silyl ether proceeded smoothly to afford 67% of **41**. Using a mixture of methyldichlorophosphate in pyridine,<sup>34</sup> pseudo-hexasaccharide cyclic phosphate could be isolated after acidic workup. The crude material was subjected to silyl ether cleavage using TBAF to give a 70% yield of **42**.



On page 13, please delete the illustration and caption shown below:

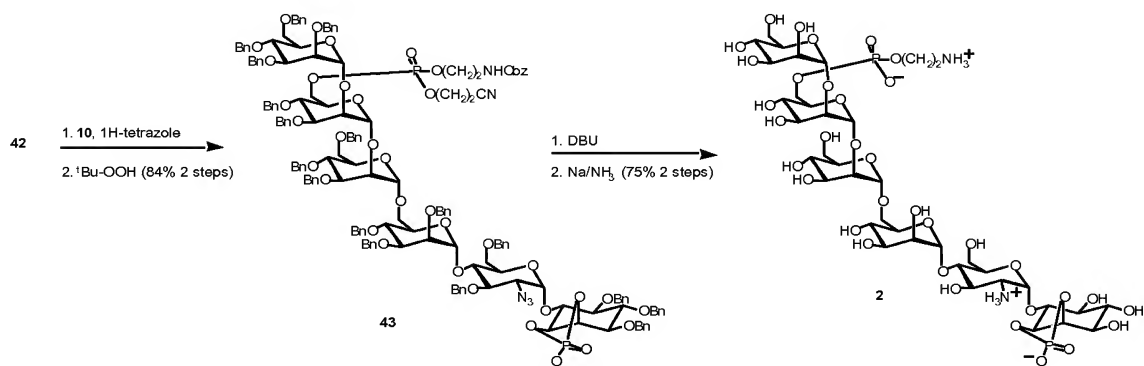


**Scheme 4.7** Synthesis of cyclic phosphate **93**

Please amend page 13, lines 9-13, as follows:

Reaction with phosphoramidite  $10^{7b}$  and oxidation provided bis-phosphate **43** as a mixture of diastereomers. DBU was used to cleave the -cyanoethoxy blocking group, and removal of the benzyl ethers, benzyloxy (Cbz) carbamate, and azide was accomplished in a single step with Na/NH<sub>3</sub> to afford desired GPI **2**. See Figure 16. The final product was characterized by <sup>1</sup>H, and <sup>31</sup>P NMR, as well as by MALDI-TOF mass spectrometry.

On page 14, please delete the illustration and caption shown below:

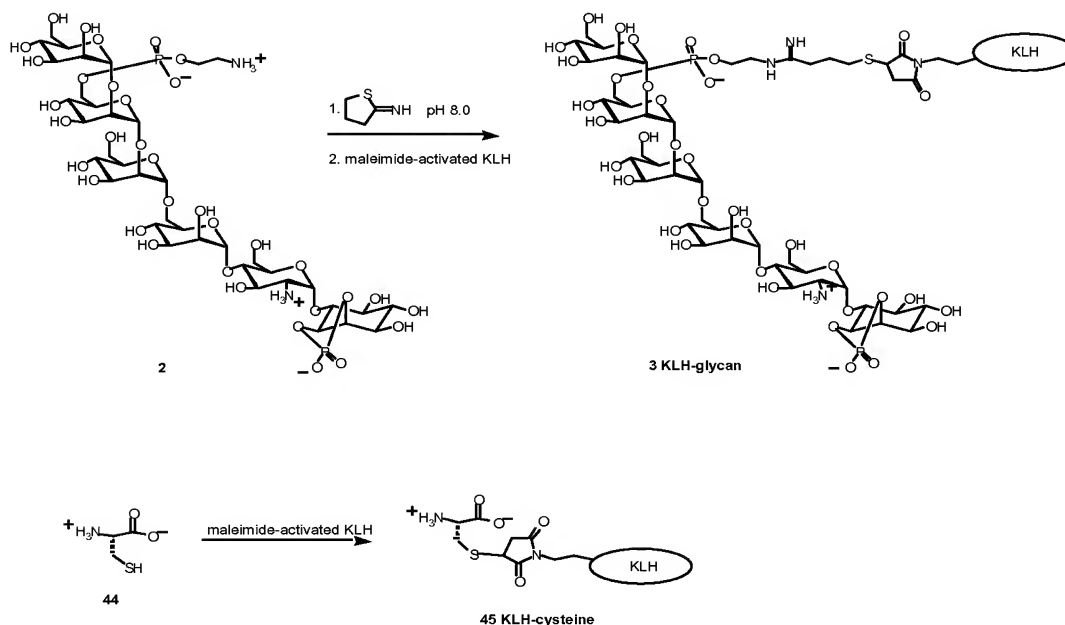


**Scheme 4.8** Synthesis of target **2**

Please amend page 14, lines 5-15, as follows:

To prepare an immunogen, the synthetic GPI glycan **3** was treated with 2-iminothiolane (Scheme 4.9 Figure 17) to introduce a sulfhydryl at the primary amine within the ethanolamine phosphate, desalted, and conjugated to maleimide-activated ovalbumin (OVA, in molar ratio 3.2:1) or Key-Hole Limpet Haemocyanin (KLH, in molar ratio 191:1), and used to immunize mice. The synthetic malarial GPI glycan was immunogenic in rodents. Antibodies from KLH-glycan **3** immunized animals gave positive IgG titres against OVA-glycan but not sham-conjugated OVA-cysteine **45** containing identical carrier and sulfhydryl bridging groups (Figure 18). No reactivity to GPI glycan was detected in pre-immune sera or in animals receiving sham-conjugated KLH. More significantly, antibodies raised against synthetic *P. falciparum* GPI glycan bound to native GPI as judged by several methods.

On page 15, please delete the illustration and caption shown below:



**Scheme 4.9** Preparation of immunogen and sham

Please amend page 15, line 4, to page 16, line 9, as follows:

The murine *P. berghei* ANKA severe malaria model has salient features in common with the human severe and cerebral malaria syndromes and is the best available small animal model of clinically severe malaria. To determine whether anti-GPI immunization prevents systemic and cerebral pathogenesis in this pre-clinical model, C57Bl6 mice primed and twice boosted with 6.5 µg KLH-glycan (0.18 µg glycan) or KLH-cysteine in Freund's adjuvant were challenged with *P. berghei* ANKA, and the course of disease monitored (~~Figure 4.4a~~ Figure 19A). 100% of both sham-immunized and naïve control mice died within 5-8 days. There were no differences between naïve and sham-immunized mice indicating exposure to carrier protein alone in Freund's adjuvant does not influence disease rates. In contrast, mice immunized with synthetic *P. falciparum* GPI glycan coupled to KLH were substantially protected against cerebral malaria, with significantly reduced death rates (75% survival, ~~Fig. 4.4a~~ Figure 19A). In four separate additional experiments, results over the range of 58.3-75% survival over this time-period in vaccine recipients (n=50 total) vs. 0-8.7% survival in sham-immunized controls (n=85) were obtained. Parasitaemias were not significantly different between test and control groups in these experiments, demonstrating that prevention of fatality by anti-GPI vaccination does not operate through effects on parasite growth rates (~~Figure 4.4b~~ Figure 19B).

Severe malaria in both humans<sup>35</sup> and rodents<sup>36</sup> may be associated with additional organ-specific and systemic symptoms, including pulmonary edema and serum acidosis. Our collaborators sought to determine whether anti-GPI vaccination protects against these additional non-cerebral disease syndromes in mice. Both sham-immunized and naïve individuals developed pronounced pulmonary edema by day 6 post-infection, as measured by lung dry:wet weight ratios, and this symptom was markedly reduced in vaccine recipients (~~Figure 4.4c~~ Figure 19C). Similarly, whereas sham-immunized and unimmunized mice developed significant acidosis as shown by reduced blood pH at day 6 post-infection, in vaccinated mice blood pH was maintained at physiological levels (~~Figure 4.4d~~ Figure 19D). Immunizing against GPI clearly prevented the development of pulmonary edema and acidosis as well as cerebral malaria in *P. berghei* infection.

On page 16, please delete the illustration and caption shown below:

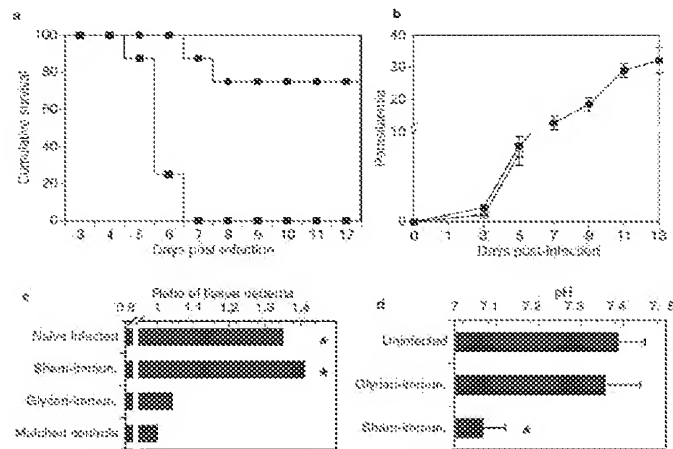


**Figure 4.4** Immunization against the synthetic GPI glycan substantially protects against murine cerebral malaria, pulmonary edema and acidosis. a) Kaplan-Meier survival plots, and b) parasitaemias, to 2 weeks post-infection, of KLH-glycan-immunized (closed circles) and sham-immunized (open squares) mice challenged with *P. berghei* ANKA; c) As an index of pulmonary edema, the ratio of wet weight to dry weight of lungs from KLH-glycan-immunized and sham-immunized animals at day 6 post-infection are expressed as a proportion of the lung wet:dry weight ratio of age/sex matched uninfected controls; d) pH of serum drawn at day 6 from uninfected and *P. berghei*-ANKA-infected immunized and sham-immunized donors.

Please amend page 17, lines 10-21, as follows:

Using our solution phase synthesis as a guide, we contemplated the automated synthesis of **2**. While it would be ideal to prepare the entire skeleton on solid-phase, the  $\alpha$ -linkage between the inositol and glucosamine residues presented a serious impediment to a fully automated synthesis. Relatively few methods are available for the preparation of 1,2-*cis* glycosidic linkages.<sup>37</sup> Previous GPI syntheses addressed this problem by either separating mixtures of isomers, or utilizing completely  $\alpha$ -selective coupling methods followed by protecting group manipulations.<sup>38</sup> Neither of these solutions was amenable to solid-phase, which led us to dissect GPI **2** into two fragments: a known disaccharide **21** not readily accessible on solid phase, and a tetra-mannosyl fragment (**46**) readily prepared using our automated solid-phase methodology (~~Figure 4.5~~ Figure 20A and Figure 20B). The two fragments could be joined using *n*-pentenyl glycoside (NPG) coupling methodology,<sup>39</sup> or via hydrolysis and conversion into tetrasaccharide trichloroacetimidate **47**.

On page 18, please delete the illustration and caption shown below:

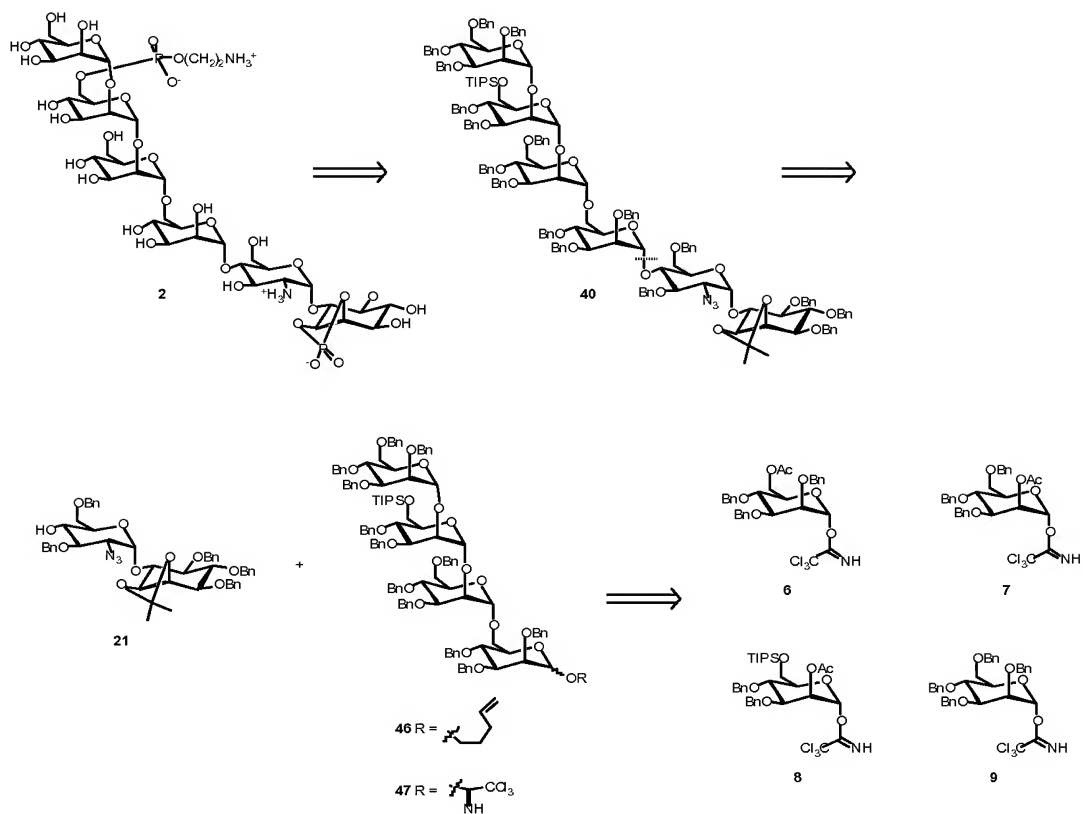


**Figure 4.5** Retrosynthesis for automated synthesis

Please amend page 18, lines 5-11, as follows:

Tetrasaccharide **46** was accessed on solid-phase using four readily available trichloroacetimidate building blocks **6-9** (~~Scheme 4.10~~ Figure 21). The automated synthesis was carried out on a modified ABI 433A peptide synthesizer using octenediol-functionlized Merrifield resin **48**. Each coupling cycle (~~Table 4.1~~ Figure 22) relied on double glycosylations to ensure high coupling efficiencies and a single deprotection event. Coupling of **6** to resin **48** using catalytic TMSOTf was followed by removal of the acetate ester upon exposure to NaOMe.

On page 19, please delete the table and caption shown below:

Function	Reagent	Time (min)
Glycosylation	5 equiv. donor and 5 equiv. TMSOTf	20
Wash	Dichloromethane	9
Glycosylation	5 equiv. donor and 5 equiv. TMSOTf	20
Wash	Dichloromethane	9
Deprotection	2 × 10 equiv. NaOMe	60
Wash	0.2 M AcOH/0.2 M MeOH/THF	9
Wash	Tetrahydrofuran	9
Wash	Dichloromethane	9

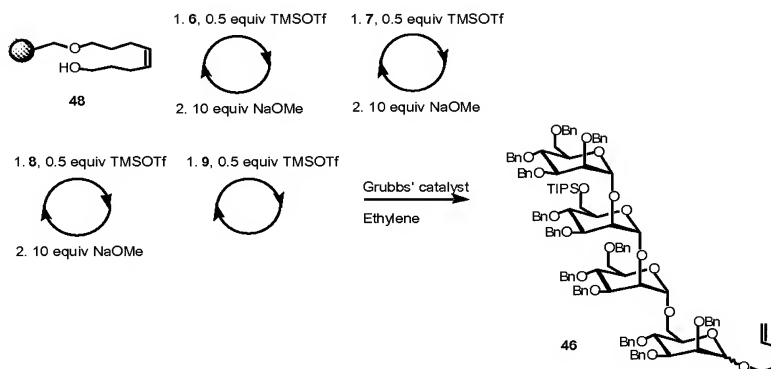
**Table 4.1** Conditions for automated synthesis of **46**



Please amend page 19, lines 3-13, as follows:

Based on a solution-phase model, we did not anticipate a selective coupling between donor **6** and the functionalized resin; the stereochemistry of this first coupling was inconsequential since the NPG resulting from the automated synthesis was to be coupled at the reducing end. Elongation of the oligosaccharide chain was achieved using monosaccharide **7**<sup>7a</sup>, followed by deprotection of the 2-O-acetate using NaOMe. Coupling of building block **8** employing catalytic TMSOTf and deprotection with NaOMe proceeded smoothly to create a resin-bound trisaccharide, before the final coupling with donor **9**.<sup>1a</sup> Cleavage of the octenediol linker using Grubbs' catalyst<sup>40</sup> under an atmosphere of ethylene provided crude *n*-pentenyl tetrasaccharide **46**. HPLC analysis of the crude reaction products revealed two major peaks (Figure 4.6 Figure 22): the desired tetrasaccharide **46** (44% relative area) and deletion sequences (15% relative area).

On page 19, please delete the illustration and caption shown below:



**Scheme 4.10** Automated synthesis of GPI **46**

Please amend page 19, line 18, to page 20, line 5, as follows:

The crude material was purified by HPLC to provide **46** as a mixture of  $\alpha$  and  $\beta$ -anomers. Prior to attempting the crucial 4+2 coupling, a model coupling between NPG-monosaccharide **49** and disaccharide **21** was carried out but failed to produce the desired product (~~Scheme 4.11~~ Figure 24). The failure of **49** as an effective glycosyl donor led us to examine glycosyl trichloroacetimidate **47** as a coupling partner. Conversion of **46** into glycosyl donor **47** proceeded smoothly over two steps. Reaction of trichloroacetimidate **47** with disaccharide **21** afforded the desired hexasaccharide **40** in modest yield.

On page 20, please delete the illustration and caption shown below:

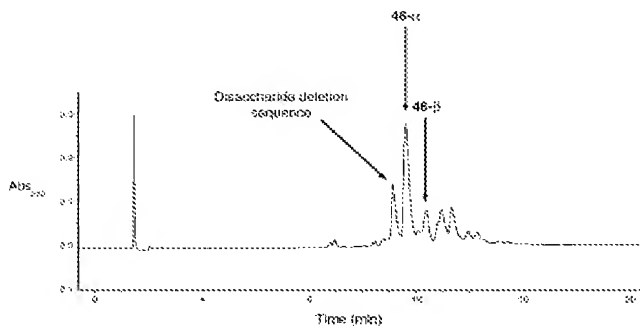
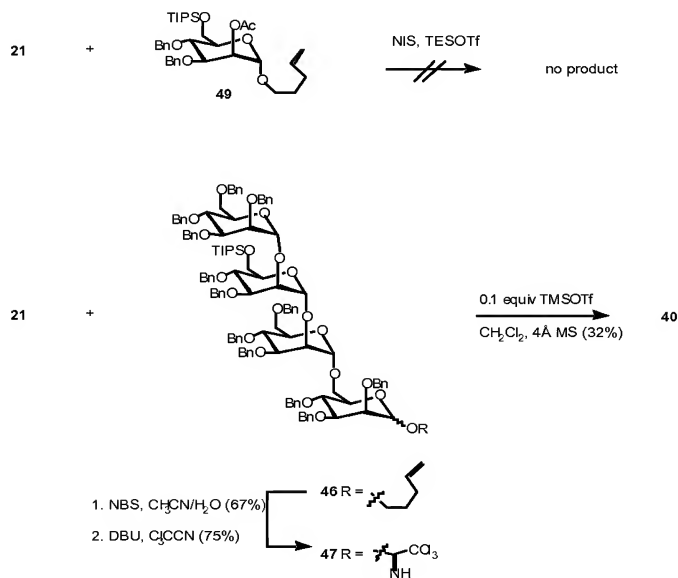


**Figure 4.6** HPLC analysis of automated synthesis of **46**. Flow rate: 1 mL/min, 5→20% EtOAc/hexanes (20 min).

On pages 20-21, please delete the illustration and caption shown below:

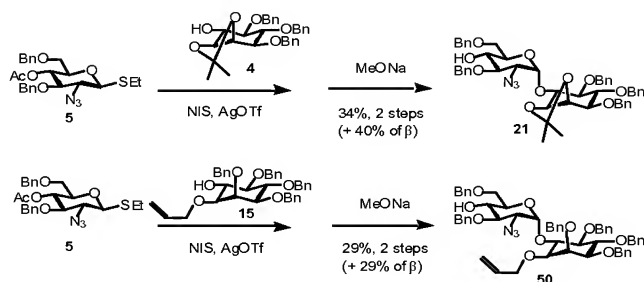


**Scheme 4.11** 4+2 coupling

Please amend page 20, lines 3-6, as follows:

To allow other phosphorylation patterns, use of the inositol acceptors with different protection patterns were necessary. Coupling acceptor **15** with thiodonor **5** under the same conditions as with acceptor **4** gave, following deacetylation, a separable anomeric mixture of disaccharide acceptors **50**. (~~Scheme 4.12~~ Figure 25).

On page 21, please delete the illustration and caption shown below:

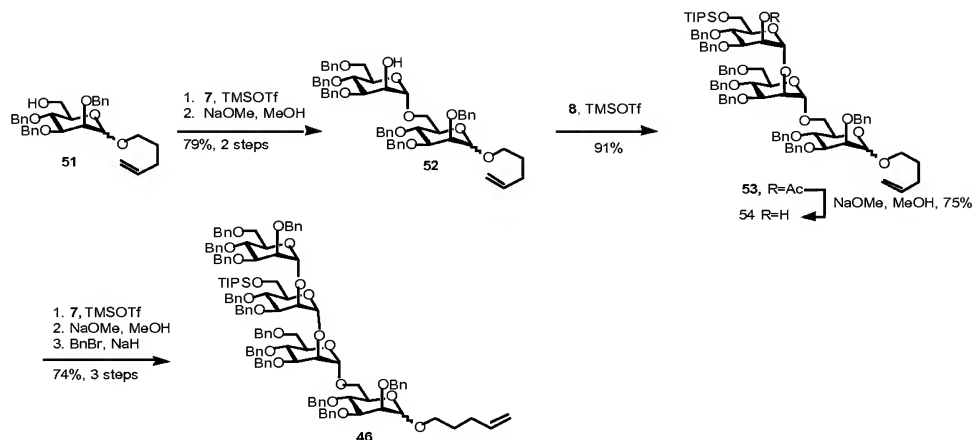


**Scheme 4.12** Differentially-protected disaccharide acceptors

Please amend page 21, lines 9-11, as follows:

Tetramannose component **46** can also be prepared in solution, if large quantities are required (~~Scheme 4.13~~ Figure 26). Sequential coupling/deprotection of donors **7**, **8**, and **7** to acceptor **51**, followed by benzylation of the free hydroxyl, gave **46** as expected.

On page 21, please delete the illustration and caption shown below:

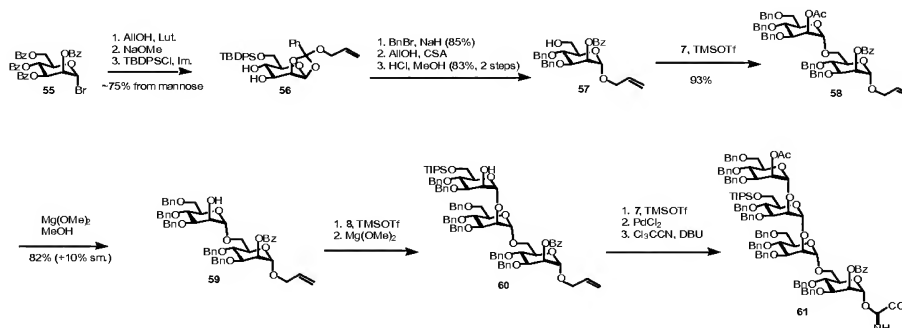


**Scheme 4.13** Solution-phase synthesis of tetramannose structure

Please amend page 21, line 14, to page 22, line 7, as follows:

The modest 4+2 coupling ~~yields~~ yields seen above are partially due to the instability of the highly-activated tribenzyl donor being used. Furthermore, mammalian GPI structures have a phosphoethanolamine on the 2-OH of the first mannose residue. Both of these issues were addressed simultaneously by the use of an ester on the 2-position of the reducing-end mannose in the tetrasaccharide donor; the presence of ester attenuates the activity of the donor, resulting in less decomposition, and it is removed to enable installation of phosphoethanolamine. Our route is shown in ~~Scheme 4.14~~ Figure 27: from known tetrabenzylmannose bromide, closure to the allyl orthoester takes place in the presence of the alcohol and 2,6-lutidine; debenzoylation and selective silylation of the primary hydroxyl gave **56** in good ~~yield~~ yield. Benzoylation was followed by opening of the orthoester (in the presence of excess allyl alcohol) and acid-catalyzed desilylation gave acceptor **57**. This was coupled to **7** under standard conditions; selective removal of the acetate ester using magnesium methoxide gave **59** in 90% yield, based on the recovery of a small amount of starting material. Polymer ~~extension~~ extension proceeded using the same techniques, and allyl removal used standard conditions, providing the new tetrasaccharide donor **61**.

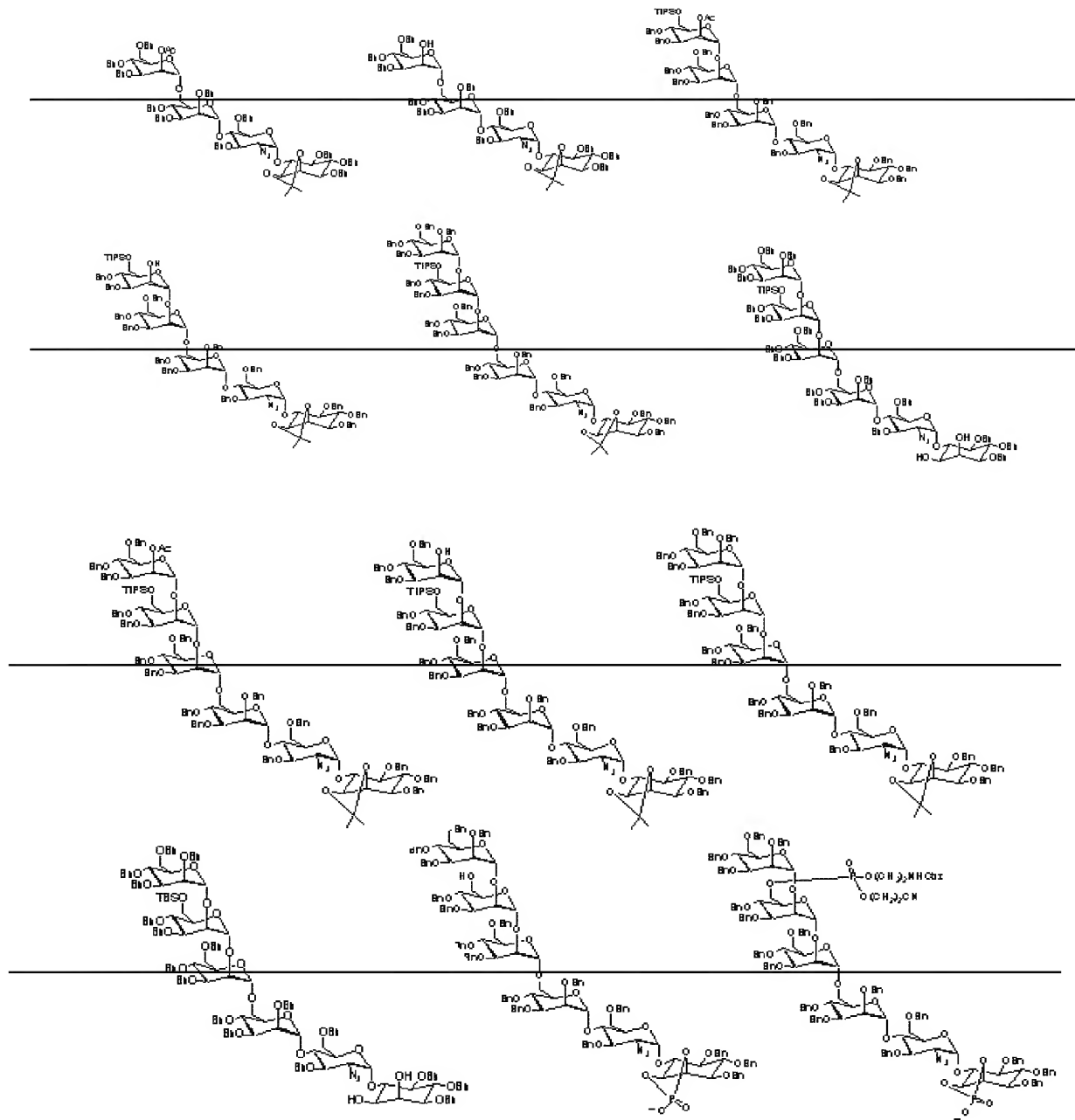
On page 22, please delete the illustration and caption shown below:

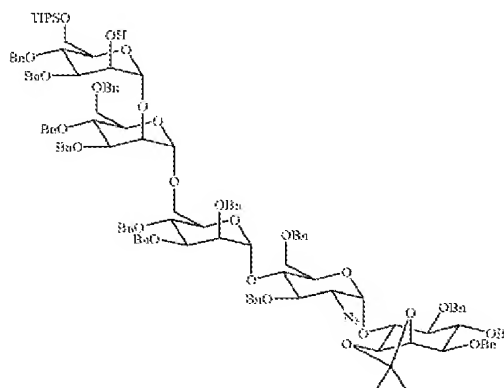
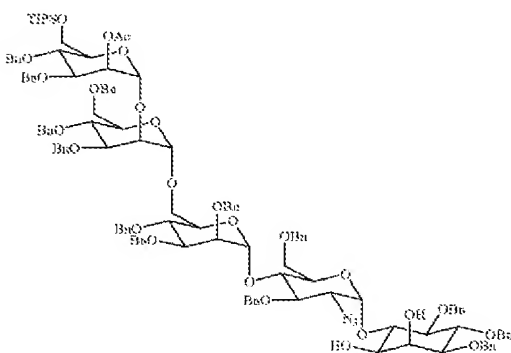
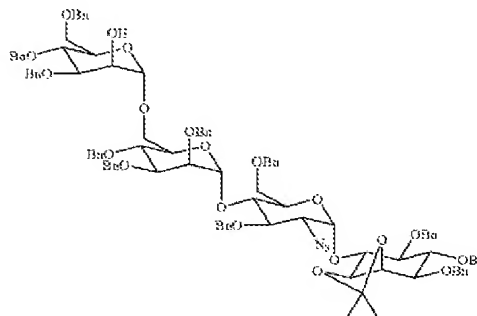
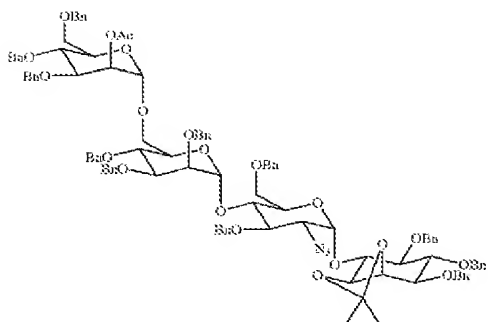
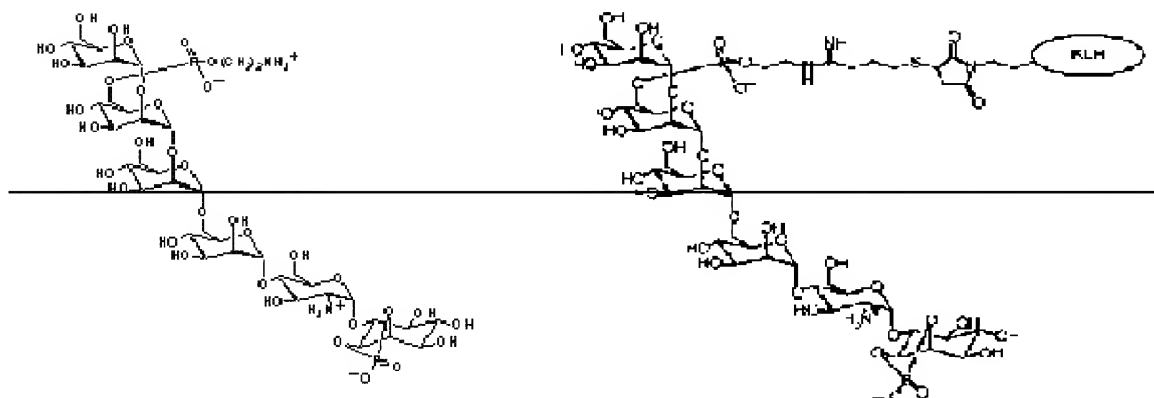


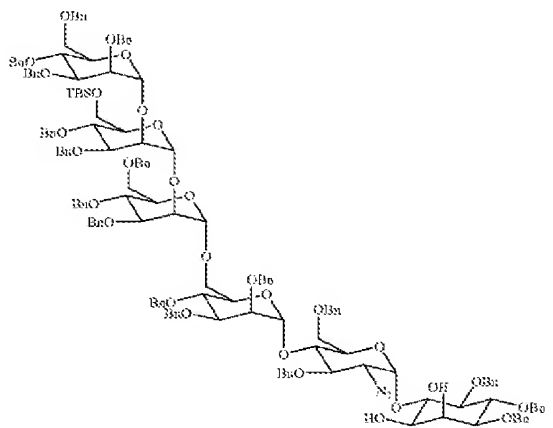
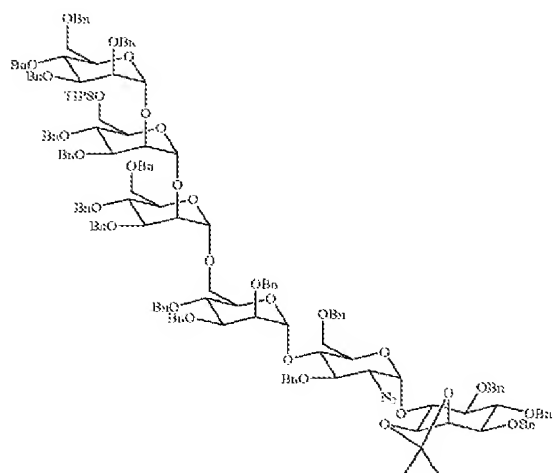
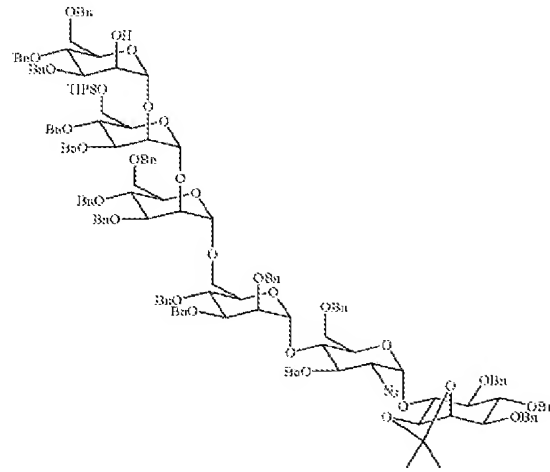
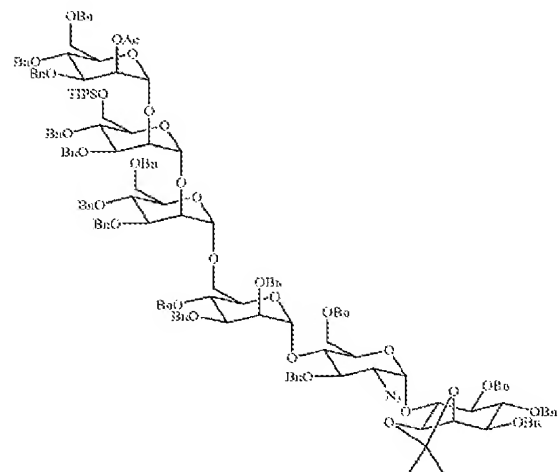
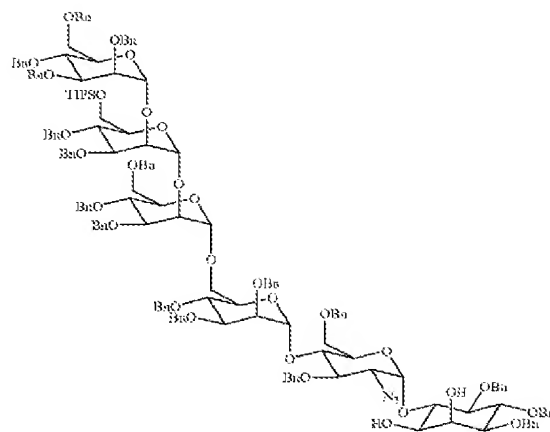
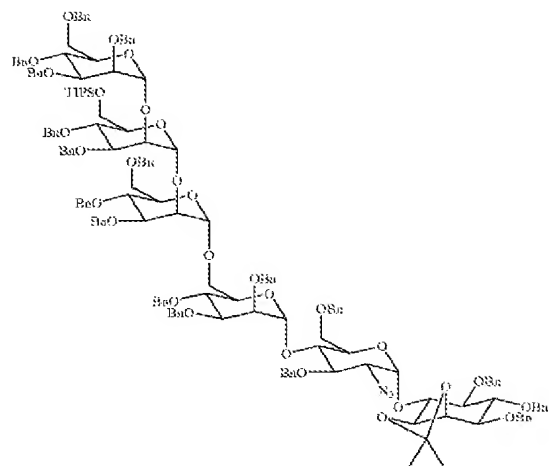
**Scheme 4.14** Synthesis of more-versatile tetramannose donor

Please amend the paragraph that begins on page 24, at line 9, and ends on page 25, line 3, as follows:

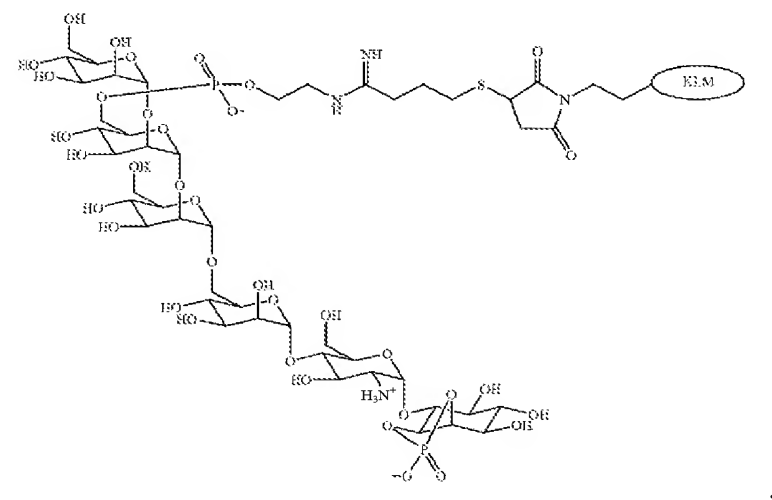
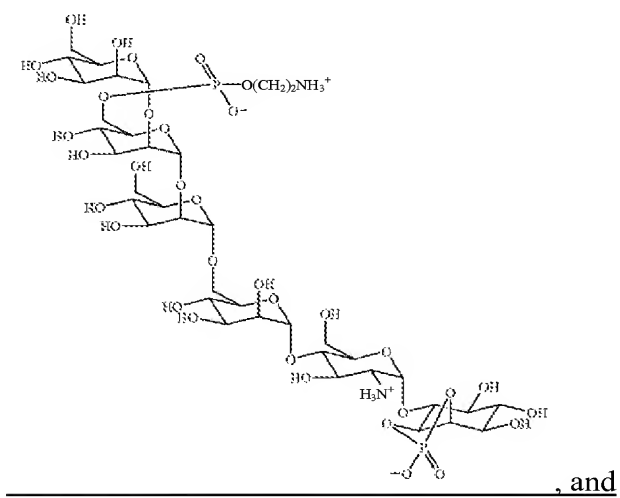
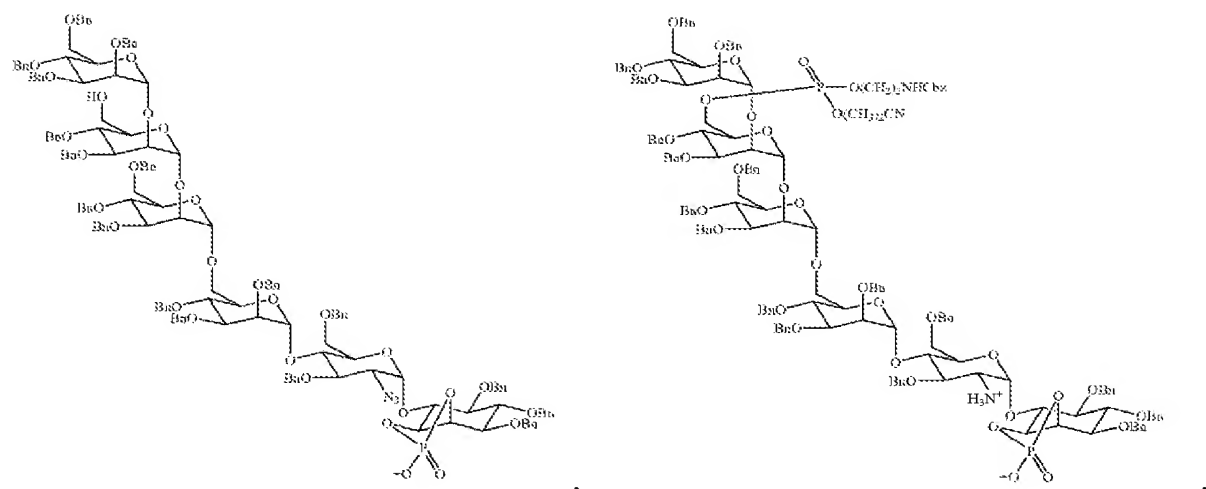
In certain embodiments, the present invention relates to the aforementioned compound, wherein said compound of formula **I** is selected from the group consisting of:





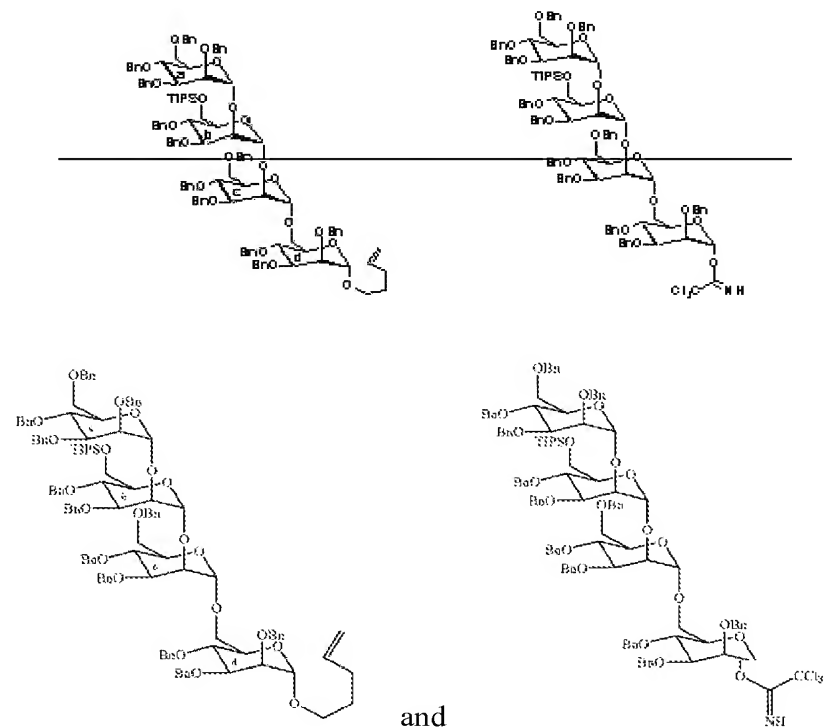






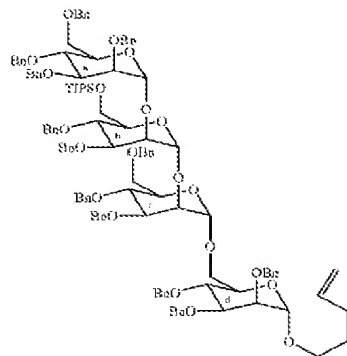
Please amend the paragraph on page 26, lines 22-24, as follows:

In certain embodiments, the present invention relates to the aforementioned compound, wherein said compound of formula **II** is selected from the group consisting of:

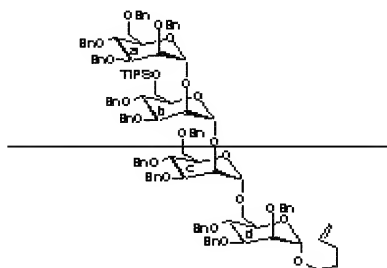


Please amend the paragraph on page 28, lines 22-25, as follows:

In certain embodiments, the present invention relates to the aforementioned method,



wherein said tetrasaccharide is \_\_\_\_\_, ~~represented by formula VI:~~



**VI**